Available online at www.sciencedirect.com
ScienceDirect
Chinese Journal of Aeronautics 22(2009) 43-48
Chinese Journal of Aeronautics
www.elsevier.com/locate/cja

# Factors Resulting in Micron Indentation Hardness Descending in Indentation Tests

Li Min[a], Chen Weimin[b,*]

[a]*School of Aeronautics Science and Engineering, Beijing University of Aeronautics and Astronautics, Beijing 100191, China*

[b]*Division of Engineering Science, Institute of Mechanics, Chinese Academy of Science, Beijing 100080, China*

Received 3 June 2008; accepted 5 September 2008

**Abstract**

Some factors that affect the experimental results in nanoindentation tests such as the contact depth, contact area, load and loading duration are analyzed in this article. Combining with the results of finite element numerical simulation, we find that the creep property of the tested material is one of the important factors causing the micron indentation hardness descending with the increase of indentation depth. The analysis of experimental results with different indentation depths demonstrates that the hardness decrease can be bated if the continuous stiffness measurement technique is not adopted; this indicates that the test method itself may also be one of the factors causing the hardness being descended.

*Keywords:* nanoindentation; hardness; indentation size effect

## 1. Introduction

With the miniaturization and micromation of materials and structures, and with the development of advanced materials, the mechanical properties of materials are increasingly measured by nanoindentation techniques. The method presented by W. C. Oliver and G. M. Pharr[1] (referring to it as O & P method) is used widely in current researches and tests. In O & P method, following I. N. Sneddon's[2] formula of elastic indentation produced by conic indenter, the indentation contact depth can be obtained. W. C. Oliver and G. M. Pharr adopted reduced modulus to include the elastic effect of the indenter and take fused silicon (aluminum was taken originally) as the calibration material. They set up an empirical formula in polynomial form to represent the contact area as a function of contact depth and determined the coefficients through an iterative process. Then, the hardness-depth curve and the elastic modulus-depth curve were obtained based on the load-displacement curve. By doing so, they avoided the use of scanning electronic microscope (SEM) to determine the indentation area, so that the efficiency was increased.

By the O & P method, many works are concerned with the phenomenon that the hardness of specimens increases with the decrease of indentation depth for the depth being below 100 nm, named as the "indentation size effect". The research on this phenomenon became hot spot in past ten years[3-11]. Some people take it as the proof of the theory of strain gradient. And the others think that the test method and test error are just the important factors causing this phenomenon. In fact, the phenomenon of the hardness changing with the indentation depth is present not only in the indentation depth being below 100 nm but also in that above 100 nm. What are the factors that result in this phenomenon? Is it due to the processing method of the experimental data or the inherent properties of the material? We try to answer these questions in this article.

There are many factors such as the tip radius of the indenter, the determination of the contact point, piling-up and sinking-in phenomena, and the effect of test method on the experimental data. In this article, by observing some factors and using the finite elements numerical simulation, it is demonstrated that the disfigurement of indenter tip and the handling of the contact depth and contact area are not the main reasons for the micron indentation hardness decreasing with the increase of indentation depth. But the creep property

*Corresponding author. Tel.: +86-10-82543891.
*E-mail address:* wmchen@imech.ac.cn
Foundation item: National Natural Science Foundation of China (10772183, 10532070)


doi: 10.1016/S1000-9361(08)60067-9

of the specimen may be one of the important factors. The experimental results for different indentation depths demonstrate that the hardness decrease can be bated if continuous stiffness measurement (CSM) method is not adopted.

## 2. Experimental Phenomena

For the convenience of presentation, we only give some of the formulas and the corresponding schematic figures and omit the detailed discussion on O & P method. Fig.1 shows a typical load-displacement curve, and Fig.2 shows the deformation of specimen under indenter.

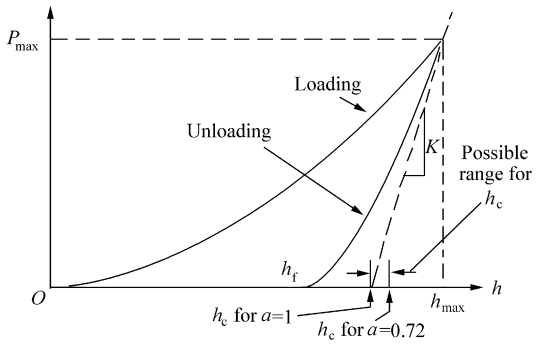


Fig.1 Load-displacement curve.

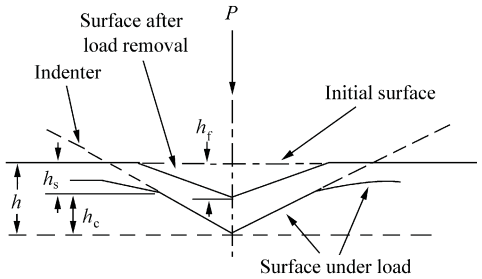


Fig.2 Deformation under the indenter.

The contact depth $h_c$, the indentation depth $h$, the load $P$, and the initial unload stiffness $S$ have the relationship as follows:

$$h_c = h - \varepsilon \frac{P}{S} \tag{1}$$

where $\varepsilon = 2 - 4/\pi = 0.727$, but in practical tests, this value is often taken as 0.750 because with this value, the theoretical results have better agreement with the experimental results. In O & P method, the contact area is assumed as follows to count in the geometrical nonperfect indenter (such as the disfigurement of indenter tips):

$$A(h_c) = 24.5h_c^2 + \sum_{i=1}^{8} c_i h_c^{1/2^{i-1}} \tag{2}$$

The definition of the hardness of nanoindentation is

$$H = \frac{P}{A} \tag{3}$$

By virtue of Eqs.(1)-(3), together with the calibrated $c_1$-$c_8$, using the experimental data $P$, $S$, $h$, the curve of hardness versus depth ($H$-$h$) can be obtained.

In this article, the nanoindentation tests are performed using a nano indenter XP manufactured by MTS Systems Corporation. The tested materials include fused silica, tungsten, copper, and aluminum. Fused silica is the calibrated material supplied by MTS Systems Corporation. The area function is:

$$A(h_c) = c_0 h_c^2 + \sum_{i=1}^{4} c_i h_c^{1/2^{i-1}} \tag{4}$$

The calibrated factors have the values of $C_0$ = 24.912, $C_1 = 261.7$, $C_2 = -279.2$, $C_3 = -25.3$, $C_4$ = 129.2. The CSM technique is used, and the strain rate is maintained constant, i.e. $\dot{\varepsilon} = 0.05$ nm/s.

Fig.3 shows the experimental $H$-$h$ curves of these four materials; the dot denotes the experimental data, and the straight line denotes the average hardness $\bar{H}$ for the depth being above 100 nm. Because the strain rate is kept constant, the number of data for small depth is larger than that for large depth, so the average value is close to the value for small depth.

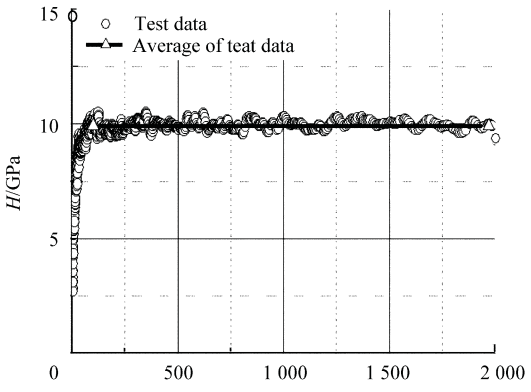


(a) Fused silica

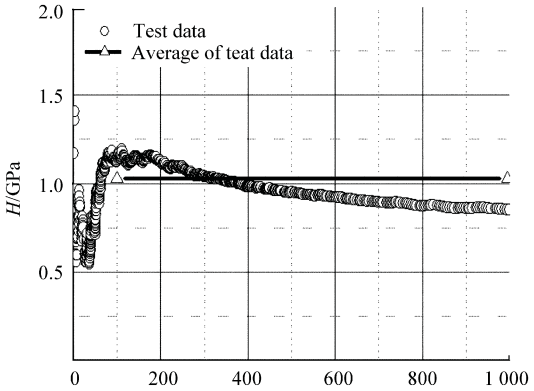


(b) Copper

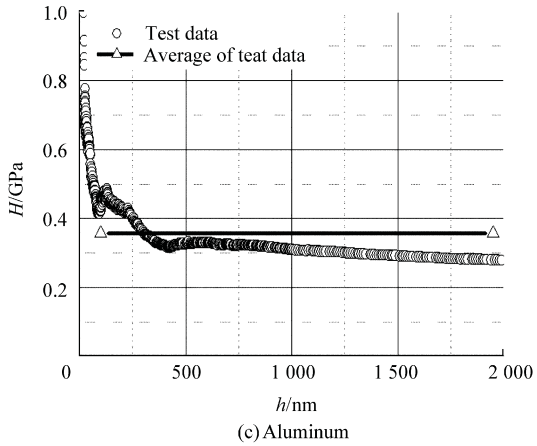


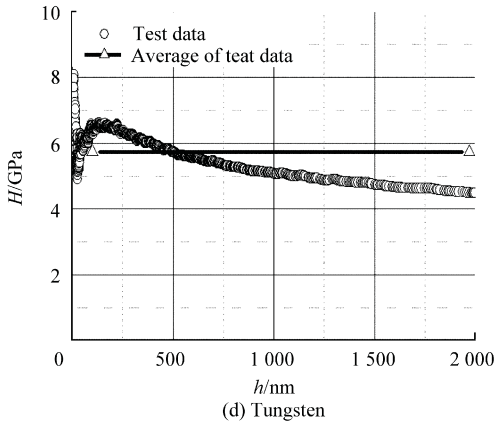


Fig.3 Curves of nanoindentation hardness versus indentation depth for four materials.

First, it can be seen that there are fluctuations in experimental data for the depth being below 100 nm affected largely by the indenter geometrical disfigurement, the determination of the contact point, the superposition of CSM dynamic displacement, and the roughness of the specimen surface, so here the experimental data for the depth being below 100 nm are not used. Observing the test data for the depth above 100 nm, we can see that for most of the materials, the hardness of micron depth is smaller than that of nanometer depth, although the decreasing degree varies with the materials. The comparison of the results of the hardness for 100 nm and 2 000 nm depths of the four materials are shown in Table 1, and the decrease ranges compared with the average hardness are also listed in Table 1.

Among the four materials, the hardness of aluminum, copper, and tungsten show decrease, and the hardness of fused silica change little. Because fused silica is the calibrated material for the O & P method, we may ask such questions: what is the reason of hardness decrease? Is the decrease introduced by the processing method of experimental data or introduced by the inherent properties of the material?

## 3. Analyses of Experimental Results

By O & P method, the experimental data are analyzed in the following ways: for every set of $P$, $S$, and $h$, according to Eqs.(1)-(3), one can obtain $h_c$, $A(h_c)$, and $H$, then the $H$-$h$ curve can be obtained. By dimensional analysis[12], for the self-similar indenters: $P \propto h^2$, and $A \propto h^2$, so $H = P/A = \text{constant}$, it means that $H$ is independent of the indentation depth. But this is not consistent with the experimental results. In the following sections, we will analyze the effects of some factors such as the contact depth, contact area, and load on the $H$-$h$ curves, so as to try to find the main factor, which causes the hardness to be decreased.

**Table 1 Comparison of indentation hardness for four materials**

| Material | 1 | | | 2 | | | 3 | | |
|---|---|---|---|---|---|---|---|---|---|
| | $H_{100}$/GPa | $H_{2000}$/GPa | Error/% | $H_{100}$/GPa | $H_{2000}$/GPa | Error/% | $H_{100}$/GPa | $H_{2000}$/GPa | Error/% |
| Fused silica | 9.96 | 9.90 | 1 | 9.89 | 9.85 | 1 | 10.31 | 10.10 | 2 |
| Aluminum | 0.42 | 0.29 | 36 | 0.37 | 0.29 | 22 | 0.44 | 0.29 | 42 |
| Copper | 1.38 | 0.93 | 41 | 1.15 | 0.85 | 29 | 1.40 | 0.87 | 49 |
| Tungsten | 6.41 | 4.49 | 33 | 6.48 | 4.58 | 33 | 5.94 | 4.56 | 25 |

Note: The largest depth for copper is 1 000 nm; Error = $(H_{100} - H_{2000})/\bar{H} \times 100\%$

### 3.1. Contact depth

Eq.(1) can be rewritten as:

$$\frac{h_c}{h} = 1 - \varepsilon \frac{P}{S}\frac{1}{h} \tag{5}$$

Together with the experimental data, the values of $h_c/h$ can be obtained and shown as Fig.4.

The average experimental values of $h_c/h$ for the four materials with their indentation depth being between 100 nm and 1 000 nm are 0.980 (aluminum), 0.970 (copper), 0.685 (fused silica), and 0.934 (tungsten), respectively. It can be seen that $h_c/h$ almost keep constant when the indentation depth is above 100 nm. Whereas among the four materials, the fused silica has the largest fluctuation. It should be noted that Eq.(1), in which $h_c/h < 1$, is not suitable for the case with piling-up in which $h_c/h > 1$. We conduct the finite element numerical simulation[13] by ABAQUS (Hibbitt, Karlsson, and Sorensen, Inc.) finite element

code. The calculation results show that the $h_c/h$ is also independent of the indentation depth. Although the results of numerical simulation sometimes show $h_c/h>1$, the experimental data obtained from O & P method show $h_c/h<1$, the consistent conclusion can be obtained that $h_c/h$ is independent of the indentation depth. That means, $h_c \propto h$.

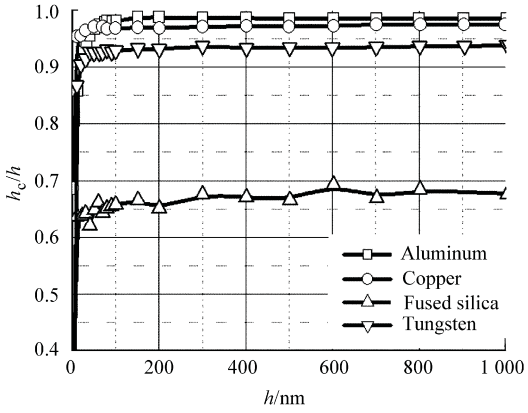


Fig.4 $h_c/h$-$h$ curves obtained by O & P method.

### 3.2. Contact area

The geometry of a real indenter cannot be perfect for the reason of manufacture. So the area function of the indenter needs to be calibrated. We take the conic indenter as an example to discuss the error introduced by the radius of the indenter tip. Fig.5 is the sketch of the indenter with $r \neq 0$. In which $\xi = r(1/\sin\alpha - 1)$ and $d = r(1-\sin\alpha)$. We set the semicone angle $\alpha$= 70.3° and consider two kinds of indentation depths:

$$A = \pi h_c(2r - h_c) \quad h_c < d \tag{6a}$$

$$A = 24.5(h_c + \xi)^2 \quad h_c > d \tag{6b}$$

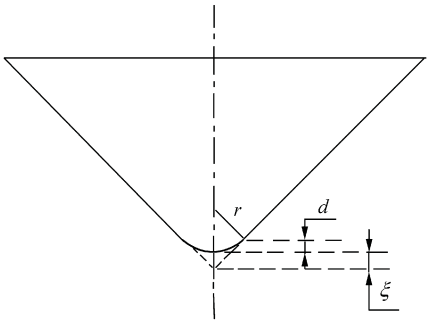


Fig.5 Sketch of a real indenter.

For the same indentation depth, the ratios of $H'$ obtained from perfect indenter area function $A = 24.5\,h_c^2$ and $H$ obtained from Eq.(6) with different $r$ are shown in Fig.6. It is seen that area error becomes larger when the indenter radius increases. That means, the greater the indenter tip radius, the greater the deviation of area function of the perfect indenter from the real area. And with the increase of indentation depth, the effect of the term related to $\xi$ in Eq.(6b) becomes smaller; hence, the area function of perfect indenter will simulate the real area more accurately. According to the calibrated factors given by the company, the ratios of the modification terms $\sum_{i=1}^{4} c_i h_c^{1/2^{i-1}}$ in Eq.(4) to the overall area are calculated and listed in Table 2. The ratio is small for the depth being above 100 nm. Even without calibrating the area, the error does not exceed 1% and 2% of the micron depth.

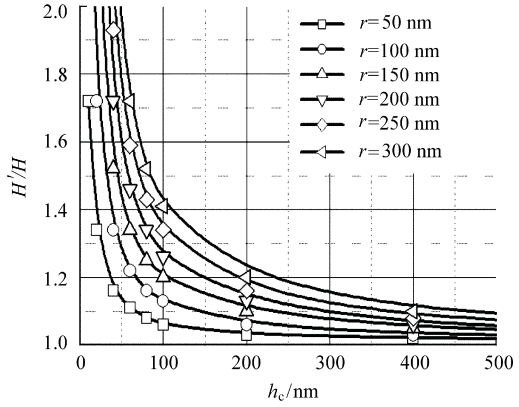


Fig.6 Error introduced by area function.

**Table 2 Ratio of the modification terms to the overall area ( ratio = $(\sum_{i=1}^{4} c_i h_c^{1/2^{i-1}})/A(h_c)$ )**

| $h_c$/mm | 100 | 200 | 300 | 400 | 500 | 600 |
|---|---|---|---|---|---|---|
| Ratio/% | 8.6 | 4.6 | 3.2 | 2.4 | 2.0 | 1.6 |
| $h_c$/mm | 700 | 800 | 900 | 1 000 | 1 500 | 2 000 |
| Ratio/% | 1.4 | 1.2 | 1.1 | 1.0 | 0.7 | 0.5 |

From the analysis of mentioned above, we can say that for the experimental data of large indentation depth, the error introduced by area calibration is small and can be ignored. According to the conclusions given in Section 2.1, we have concluded that for large indentation depth, the $A(h_c) \propto h_c^2 \propto h^2$ hold. That means even though the geometry of the indenter is not perfect, but within the micron depth region, the formula $A(h_c) \propto h^2$ can be still satisfied.

### 3.3. Load

For the $P$-$h$ curves of four materials, according to the relational expression of $P = ah^b$ and performing fitting, the values of exponent $b$ are obtained as shown in Table 3. We also give the $b$ values for the curves of the depth being above 100 nm so as to eliminate the fluctuations for small depth.

**Table 3 Fitting exponents *b* for load-displacement curves**

| Material | Fused silica | | Aluminum | | Copper | | Tungsten | |
|---|---|---|---|---|---|---|---|---|
| Test No. | Case 1 | Case 2 | Case 1 | Case 2 | Case 1 | Case 2 | Case 1 | Case 2 |
| 1 | 1.982 | 1.982 | 1.789 | 1.789 | 1.886 | 1.888 | 1.820 | 1.820 |
| 2 | 1.972 | 1.972 | 1.855 | 1.855 | 1.829 | 1.828 | 1.814 | 1.813 |
| 3 | 1.980 | 1.980 | 1.695 | 1.695 | 1.826 | 1.827 | 1.837 | 1.837 |

Notes: Case 1 means $h$ = 0-2 000 nm ; Case 2 means $h$ = 1 00-2 000 nm

It can be seen in Table 3 that whatever the experimental data for the depth being below 100 nm are included or not, only the $b$ values of fused silica are close to 2.0 (the error is about 1%), and for other three materials, the $b$ values change from 1.6 to 1.9 (the error is between 5% and 20%). It means that the relationship between the load and the displacement of fused silica almost satisfy the relation of $P \propto h^2$, but for other three materials, the relation $P \propto h^2$ is not satisfied. So according to Eq.(3), the hardness $H$ depends on the depth $h$. Because $b < 2.0$, hardness should decrease with the increase of depth, the degree of the decrease is dependent on the departure of $b$ from the value of 2.0.

### *3.4. Factor causing value b departing from 2.0*

In order to analyze the effect of the indenter tip on the load-displacement curve, the finite element numerical simulation of perfect indenter ( $r = 0$ ) and imperfect indenter ( $r = 100$ nm ) are conducted, respectively. The material property of specimen is taken as $\sigma = \varepsilon^n$. The values of exponent $b$ in $P = ah^b$ for the load-displacement curves (for indentation depth $h$ = 0-1 000 nm) are listed in Table 4. It should be noted that if only the data of the depth being below 100 nm is used, there are obvious differences between the two sets of the $b$.

**Table 4 Fitting exponents *b* obtained by numerical simulation**

| $n$ | 0.1 | 0.2 | 0.3 | 0.4 | 0.5 | 1.0 |
|---|---|---|---|---|---|---|
| $r$ = 0 | 2.007 | 1.981 | 2.017 | 1.999 | 2.020 | 2.047 |
| $r$ = 100 nm | 1.992 | 1.972 | 1.999 | 1.985 | 1.984 | 2.031 |
| Error/% | 0.75 | 0.46 | 0.90 | 0.70 | 1.80 | 0.78 |

Note: error = $|b_0 - b_{100}| / \bar{b} \times 100\%$

It is seen that the largest error introduced by the tip radius of indenter does not exceed 2%. This implies that for micron indentation depth, the tip radius of indenter almost does not affect the formula $P \propto h^2$ being satisfied. The tip radius of indenter is not the important factor causing $b$ departing from 2.0.

According to the test rule, a load holding process (about 15 s) is required when the load reaches the maximum value. The changes of indentation depth ($\Delta h$) in this process and the corresponding loads are listed in Table 5. We can see that except for fused silica, the $\Delta h$ of other three materials are as large as 40-70 nm, this may be due to the creep property of the material. The creep property can affect the loading process and its effect depends on the loading time and quantity. So the creep property may be one of the factors causing $b < 2.0$.

**Table 5 Depth change $\Delta h$ and the corresponding load during load holding**

| Material | Fused silica | Aluminum | Copper | Tungsten |
|---|---|---|---|---|
| $\Delta h$/nm | 4-6 | 35-40 | 25-40 | 50-70 |
| $P$/mN | 450.0 | 24.5 | 78.4 | 400.0 |

It is known that surface contamination can also cause the hardness decrease with the increase of indentation depth. In order to distinguish the effect of surface contamination, the nanoindentation tests for different indentation depth are conducted.

These nanoindentation tests are implemented with copper sample. The largest indentation depths are 100, 200, 300, 500, 600, 800, 1 000 nm. The experimental load-displacement curves are shown in Fig.7. The curve of nanohardness versus indentation depth is shown in Fig.8, where the dots represent the hardness for different indentation depths after load holding, and the solid line represents the continuous hardness versus the indentation depth generated by CSM. It is seen that for the same indentation depth, the hardness after load holding is lower than that generated by CSM. Hence, in addition to surface contamination, the creep property can lead to the hardness decrease.

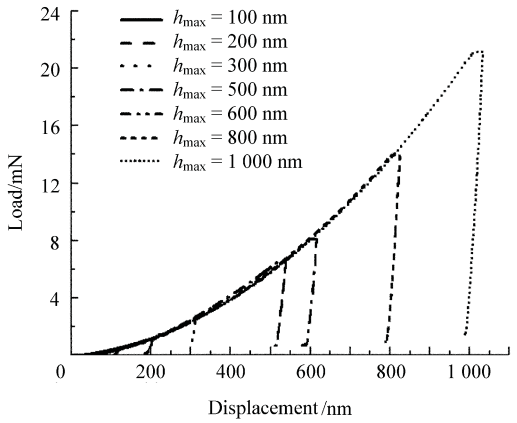


Fig.7 Load-displacement curves with different depth.

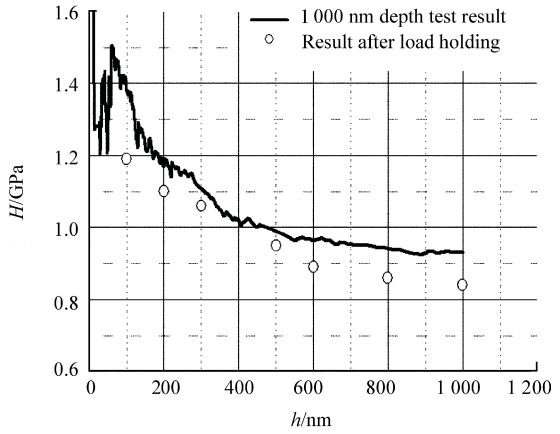


Fig.8 Hardness with different experiment method.

In indentation tests, it is often required to load and unload for many times and hold the load, so the effect of material creep can be reduced and more accurate experimental data can be obtained. But when O & P method with CSM is used, one cannot load and unload for many times. Hence, the effect of specimen creep becomes noticeable especially when the specimen has a significant creep property.

## 4. Conclusions

In the nanoindentation tests using O & P method, the indentation hardness of material decreasing with the increasing of the indentation depth brings many discussions. In this article, after analyzing the effects of the contact depth, contact area, load, and loading time on the experimental data, we have drawn the following conclusions:

(1) For micron depth, the relationship between the contact depth and the indentation depth satisfies $h_c / h =$ constant. The contact area satisfies $A(h_c) \propto h^2$ even though the tip radius of the indenter exists.

(2) The values of $b$ in $P = ah^b$ for the load- displacement curves are all smaller than 2.0, and load $P$ does not yet satisfy $P \propto h^2$ except for that of fused silica. This is one of the important reasons making the hardness decrease.

(3) The creep property of the material is one of the factors that make the hardness decrease. The geometry disfigurement of the indenter only has a limited effect. When O & P method with CSM is used, the experimental results will be certainly affected by the creep property of the specimen.

## Acknowledgment

The authors gratefully acknowledge Zhang Taihua in Institute of Mechanics, CAS for providing the test data.

## References

[1] Oliver W C, Pharr G M. An improved technique for determining hardness and elastic modulus using load and displacement sensing indentation experiments. J Mater Res 1992; 7(6): 1546-1583.
[2] Sneddon I N. The relation between load and penetration in the axisymmetric boussinesq problem for a punch of arbitrary profile. Int J Engng Sci 1965; 3(1): 47-57.
[3] Iost A, Bigot R. Indentation size effort: reality or artefact. J Mater Sci 1996; 31(13): 3573-3577.
[4] Begley M R, Hutchinson J W. The mechanics of size dependent indentation. J Mech Phys Solids 1998, 46(10): 2049-2068.
[5] Ma Q, Clarke R. Size dependent hardness of silver single crystals. J Mater Res 1995; 10(4): 853-863.
[6] Shu J Y, Fleck N A. The prediction of a size effect in microindenteation. Int J Solids and Structures 1998; 35(13): 1363-1383.
[7] Sangwal K. On the reverse indentation size effect and micro-hardness measurement of solids. Materials Chemistry and Physics 2000; 63(2): 145-152.
[8] Peng Z J, Gong J H, Miao H Z. On the description of indentation size effect in hardness testing for ceramics: analysis of the nanoindentation data. J of the European Ceramic Society 2004; 24(8): 2193-2201.
[9] Swadener J G, George E P, Pharr G M. The correlation of the indentation size effect measured with indenters of various shape. J of the Mechanics and Physics of Solids 2002; 50(4): 681-694.
[10] Kim J Y, Lee B W, Read D T, et al. Influence of tip bluntness on the size-dependent nanoindentation hardness. Scripta Materialia 2005; 52(5): 353-358.
[11] Durst K, Backes B, Goken M, Indentation size effect in metallic materials: correcting for the size of the plastic zone. Scripta Materialia 2005; 52(11): 1093-1097.
[12] Cheng Y T, Cheng C M, Scaling approach to conical indentation in elastic-plastic solids with work hardening. J of Applied Physics 1998; 84(3): 1284-1291.
[13] Chen W M, Li M, Zhang T H, et al, Influence of indenter tip roundness on hardness behavior in nanoindentation. Materials Science and Engineering: A 2007; 445-446: 323-327.

## Biography:

**Li Min** An associate professor in School of Aeronautic Science and Engineering, Beijing University of Aeronautics and Astronautics. His main research interests are smart materials and structure, aeroelastic, nanoindentation test and simulation.
E-mail: limin@buaa.edu.cn